*Am. J. Hum. Genet. 63:1439–1447, 1998*

# A Novel Locus (*RP24*) for X-linked Retinitis Pigmentosa Maps to Xq26-27

Linn Gieser,[1,*] Ricardo Fujita,[1,*,†] Harald H. H. Göring,[3] Jurg Ott,[4] Dennis R. Hoffman,[5] Artur V. Cideciyan,[6] David G. Birch,[5] Samuel G. Jacobson,[6] and Anand Swaroop[1,2]

Departments of [1]Ophthalmology and [2]Human Genetics, W. K. Kellogg Eye Center, University of Michigan, Ann Arbor; [3]Department of Genetics and Development, Columbia University, and [4]Laboratory of Statistical Genetics, Rockefeller University, New York; [5]Retina Foundation of the Southwest, Dallas; and [6]Department of Ophthalmology, Scheie Eye Institute, University of Pennsylvania, Philadelphia

## Summary

**Two genetic loci, *RP2* and *RP3*, for X-linked retinitis pigmentosa (XLRP) have been localized to Xp11.3-11.23 and Xp21.1, respectively. *RP3* appears to account for 70% of XLRP families; however, mutations in the *RPGR* gene (isolated from the RP3 region) are identified in only 20% of affected families. Close location of XLRP loci at Xp and a lack of unambiguous clinical criteria do not permit assignment of genetic subtype in a majority of XLRP families; nonetheless, in some pedigrees, both *RP2* and *RP3* could be excluded as the causative locus. We report the mapping of a novel locus, *RP24*, by haplotype and linkage analysis of a single XLRP pedigree. The *RP24* locus was identified at Xq26-27 by genotyping 52 microsatellite markers spanning the entire X chromosome. A maximum LOD score of 4.21 was obtained with DXS8106. Haplotype analysis assigned *RP24* within a 23-cM region between the DXS8094 (proximal) and DXS8043 (distal) markers. Other chromosomal regions and known XLRP loci were excluded by obligate recombination events between markers in those regions and the disease locus. Hemizygotes from the RP24 family have early onset of rod photoreceptor dysfunction; cone receptor function is normal at first, but there is progressive loss. Patients at advanced stages show little or no detectable rod or cone function and have clinical hallmarks of typical RP. Mapping of the *RP24* locus expands our understanding of the genetic heterogeneity in XLRP and will assist in development of better tools for diagnosis.**

Received July 17, 1998; accepted for publication August 31, 1998; electronically published October 16, 1998.

Address for correspondence and reprints: Dr. Anand Swaroop, W. K. Kellogg Eye Center, University of Michigan, 1000 Wall Street, Ann Arbor, MI 48105. E-mail: swaroop@umich.edu

[*] These two authors contributed equally to this work.

[†] Present affiliation: Facultad de Medicina Humana, Universidad San Martín de Porres, Lima, Peru.



0002-9297/98/6305-0022$02.00

## Introduction

Retinitis pigmentosa (RP) is a heterogeneous group of retinal degenerative disorders. Hallmarks of these diseases include night blindness, progressive loss of peripheral vision, and pigmentary changes in the retina, eventually leading to complete loss of vision (Heckenlively 1988). There is tremendous genetic and allelic heterogeneity in RP; >25 responsible loci/genes have been mapped and/or characterized (RetNet database). The first locus for an X-linked form of RP (XLRP), called "*RP2*" (RP type 2), was localized by linkage to a DNA marker, DXS7 (Bhattacharya et al. 1984), and later was refined to Xp11.3-11.23 within a 4–5 cM region (Thiselton et al. 1996). Genetic heterogeneity in XLRP was demonstrated by mapping of the second locus, *RP3* (RP type 3), at Xp21.1 (reviewed in Aldred et al. 1994*a*; Fujita and Swaroop 1996). Multilocus homogeneity tests had established *RP3* as the major XLRP locus and had suggested the existence of another locus, *RP6* (RP type 6) at Xp21.3 (Musarella et al. 1990; Ott et al. 1990). The *RP15* (RP type 15) locus was mapped to Xp22.13-22.11 by linkage analysis of a single family with a variant form of RP (McGuire et al. 1995). Genetic studies from many laboratories have demonstrated that the *RP3* subtype may account for 60%–90% of affected XLRP families (Musarella et al. 1990; Ott et al. 1990; Teague et al. 1994; Fujita et al. 1997). The *RPGR* (RP GTPase regulator) gene was recently determined to be in the *RP3* region, by use of a positional cloning strategy (Meindl et al. 1996; Roepman et al. 1996). However, extensive mutation screening has revealed *RPGR* mutations in only 20% of XLRP (and genetically characterized *RP3*) families (Buraczynska et al. 1997; Fujita et al. 1997; M. Guevara-Fujita, S. Fahrner, and A. Swaroop, unpublished data), suggesting additional genetic heterogeneity. The *RP2* gene has also been cloned recently, and mutations in this gene may account for an additional 15%–20% of XLRP families (Schwahn et al. 1998).

Previously, linkage and heterogeneity analyses were performed by the genotyping of markers spanning the short arm of the X chromosome, and statistical analysis was employed to determine the relative frequency of *RP2*

and *RP3* subtypes in XLRP families (Musarella et al. 1990; Ott et al. 1990; Teague et al. 1994). Aldred et al. (1994*b*) had reported three RP families with apparent X-linked inheritance that were not linked to the *RP2* and *RP3* loci. In our haplotype analysis of 38 XLRP families, the *RP3* locus could be unambiguously assigned to only 11 pedigrees, when obligatory recombination events were utilized to distinguish the *RP3* locus from the *RP2* locus (Fujita et al. 1997). All the known loci were excluded as the disease locus in three XLRP families that we studied. We report the localization of a novel XLRP locus to Xq26-27, in a single pedigree, by haplotype and linkage analyses of genetic markers spanning the entire X chromosome, and we describe the associated clinical phenotype. This new locus has been designated *"RP24"* (RP type 24) by the Human Genome Organization/Genome Database Nomenclature Committee.

## Subjects and Methods

### *Subjects*

Members of a five-generation family with RP (XLRP-114; fig. 1) were included in this study. Medical records of ocular examinations on patients were obtained, and a subset of patients was examined with visual-function tests. The pedigree indicated an X-linked mode of inheritance of disease, with severely affected men, no male-to-male transmission, and mildly affected or clinically asymptomatic obligate carrier women. All participants in the study were fully informed of the nature of the procedures, and the research was performed in accordance with institutional guidelines and the Declaration of Helsinki.

### *Visual-Function Tests*

Kinetic and static threshold perimetry was performed as described elsewhere (Jacobson et al. 1989, 1991, 1997). Sensitivity losses for rods (500 nm stimulus, dark adapted) and long/middle wavelength (L/M) cones (600 nm stimulus, light adapted) were calculated on the basis of locus-specific normal values. Full-field electroretinograms (ERGs) were performed with similar methods, in two centers (Retina Foundation of the Southwest, Dallas and Scheie Eye Institute, Philadelphia), by use of bipolar contact-lens electrodes and computer-based systems (Birch and Fish 1987; Jacobson et al. 1989, 1997). In three affected young males, high–stimulus energy (up to 4.6 log scotopic troland seconds [scot.td.s] blue and 4.1 log photopic troland seconds [phot.td.s] red, in Philadelphia, and up to 4.1 log phot.td.s white, in Dallas) photoresponses were recorded under dark-adapted (Philadelphia) and light-adapted (Philadelphia and Dallas) conditions. The leading edge of the photoresponses was analyzed by use of physiologically based models of phototransduction, and maximum amplitude ($R_{max}$) and sensitivity parameters were estimated for rods and cones (Cideciyan and Jacobson 1993, 1996; Cideciyan et al. 1998; Hood and Birch 1993, 1995, 1997).

### *DNA Analysis*

Blood samples were collected from participating individuals, and DNA was extracted by standard procedures. Fifty-two microsatellite markers, spanning the entire X chromosome, were used for genotyping 21 family members (including seven affected males), who represent four generations of the XLRP-114 pedigree. Descriptions of the polymorphic markers, genetic distances, and PCR conditions were obtained from Généthon and/or the Genome Database.

### *Linkage Analysis*

Two-point and multipoint (five-point) linkage analyses were performed by use of the MLINK and ILINK programs of the FASTLINK computer package (Lathrop et al. 1984; Becker et al. 1998). Linkage analysis was performed by assuming a fully penetrant disease model without phenocopies. The affected twin brothers (IV-3 and IV-4) were coded as DZ, on the basis of information provided by the family. Obligate carrier females were coded as heterozygotes; therefore, a codominant disease model essentially was used. Three of the females in the pedigree (III-10, III-11, and III-12; fig. 1) were treated as phenotypically unknown, since they were not clinically examined. The frequency of the disease-predisposing allele was set to .0001. In the two-point analysis, the marker-allele frequencies were treated as nuisance parameters—that is, the likelihood was maximized over these parameters independently, under the null hypothesis of no linkage and under the alternative hypothesis of linkage (Terwilliger and Ott 1994).

## Results

### *Exclusion of Previously Reported XLRP Loci*

Our a priori hypothesis was that a mutation in one of the previously characterized loci at Xp (*RP15, RP6, RP3,* or *RP2*) would be responsible for the disease in the XLRP-114 family. However, the haplotype analysis revealed obligatory meiotic recombination events between the disease locus and markers from the region of the aforementioned XLRP loci (fig. 1; see fig. 2 for the location of disease and marker loci). As expected from the haplotypes, the two-point linkage analysis with markers at Xp provided negative LOD scores (table 1), which excluded all known XLRP loci as the site of disease-causing mutation in this family. Markers linked to loci for other retinal disorders—such as those for congenital stationary night blindness loci, at Xp21.1-p11.2,

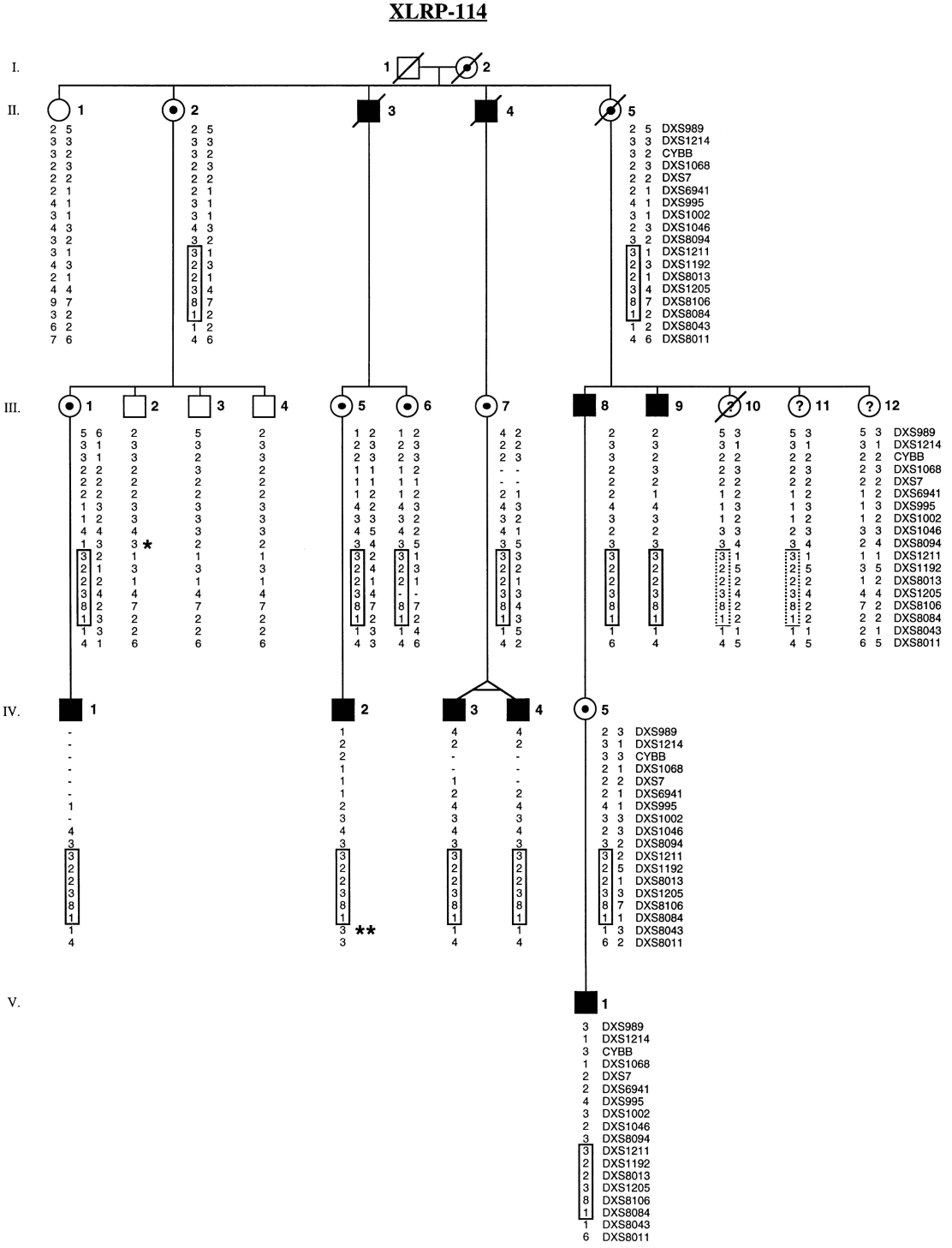


**Figure 1** Pedigree of the XLRP-114 family, showing marker haplotypes in the *RP24* region. Marker haplotypes were organized by allowance of minimum crossover events. Additional microsatellite markers from the region of known XLRP loci at Xp (*RP15*, *RP6*, *RP3*, and *RP2*) and choroideremia (*CHM*) are indicated (see fig. 2 for schematic representation). Marker loci are in the following correlative order, from DXS989 at Xp22.13 (*top*) to DXS8011 at Xq28 (*bottom*): Xpter-DXS989 (*RP15*)-DXS1214 (*RP6*)- *CYBB-RP3/RPGR*-DXS1068-DXS7-(*RP2*)-DXS6941-Cen-DXS995-DXS1002 (*CHM*)-DXS1046-DXS8094-DXS1211-DXS1192-DXS8013-DXS1205-DXS8106-DXS8084-DXS8043-DXS8011-Xqter (see fig. 2). Only pedigree members relevant for the analysis are shown. An asterisk (*) and a double asterisk (**) indicate recombination events that define the proximal and distal boundaries of the *RP24* locus, respectively. The haplotype segregating with the disease locus is boxed. Three female individuals (III-10, III-11, and III-12; indicated by a circle with a question mark [?] inside the circle) were not clinically evaluated; of these, III-10 and III-11 carry the disease haplotype (boxed with dotted lines).

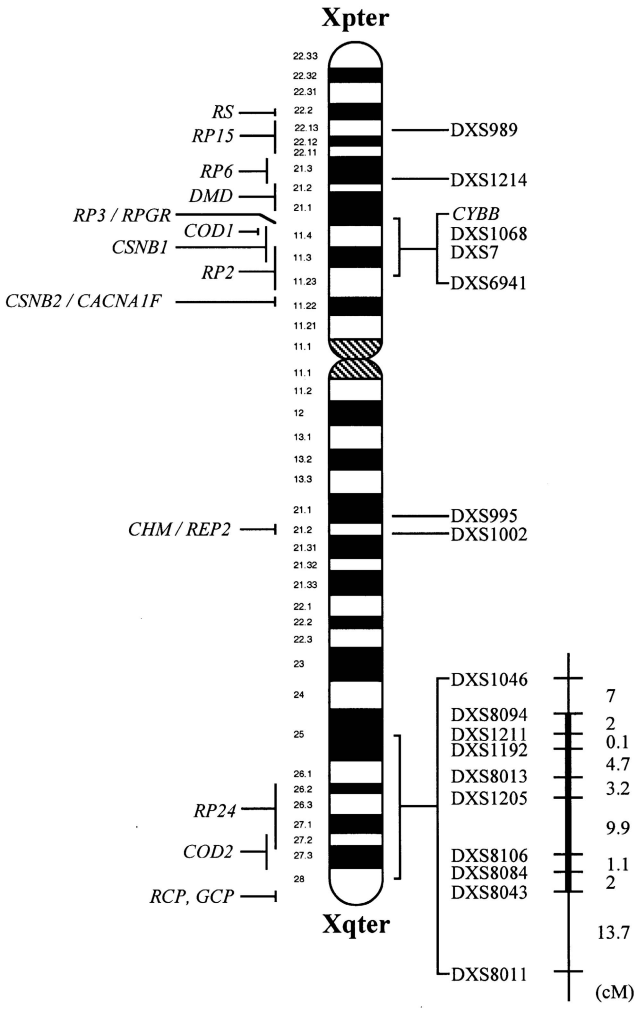


**Figure 2** Schematic representation of the human X chromosome, showing genetic loci for retinal diseases (*left*) and relevant marker loci (*right*). An expanded map of the critical genetic interval for *RP24* is shown with the thick vertical bar, and genetic distances are indicated in centimorgans (to the right of the marker loci). The map locations of disease loci were obtained from the Online Mendelian Inheritance in Man and RetNet databases.

retinoschisis, at Xp22, and choroideremia, at Xq21—were also tested and demonstrated no evidence of linkage.

### *Mapping of a Novel XLRP Locus at Xq*

A systematic genotype analysis was then undertaken with microsatellite markers, separated by 5–20 cM, spanning the remaining regions of the X chromosome. The disease status in the XLRP-114 family came into phase as markers from the Xq26-q27 region were examined (figs. 1 and 2). Two-point linkage analysis gave positive and significant LOD scores at a recombination fraction ($\theta$) of .00 for several markers in this region (DXS1211–DXS8084) (table 2). The LOD scores were within the range 0.58–4.21, solely depending on the informativeness of the marker, with a maximum LOD score ($Z_{max}$) at $\theta = .00$ for DXS8106 (table 2). In agreement with the two-point results, multipoint analysis gave a very flat LOD-score curve that was slightly >4, over this nonrecombinant interval (data not shown).

Marker haplotypes were used to determine the maximum genetic interval, as defined by recombination events in clinically affected or unaffected male individuals in the pedigree. As shown in figure 1, DXS8094 and DXS8043 (separated by 23 cM; see fig. 2 for the genetic distance between markers) identify the proximal and distal boundaries of the novel XLRP locus, which has been designated "*RP24*" by the HUGO/GDB Nomenclature Committee. In family XLRP-114, no meiotic crossovers were observed with the nine markers in the region DXS1211–DXS8084.

### *Phenotype*

Five affected males were examined by visual-function tests. Two young patients (IV-3 and IV-4) were followed during ages 5–16 years; one patient (V-1) was evaluated at age 11 years, and two older patients (III-8 and II-4) were assessed in the 6th decade of life. At age 11 years, patient V-1 had a normal eye examination and normal kinetic perimetry (targets V and I; fig. 3*A, left panel*). Static threshold perimetry showed a relatively uniform loss of rod sensitivity across the visual field (mean field loss of ~2 log units), whereas L/M cone sensitivity was within normal limits, at most test loci (fig. 3*A, middle and right panels*). Kinetic perimetry in patient IV-3, at age 8 years, was also full (target III). The two older affected males (III-8 and II-4) had typical pigmentary retinopathy and only a residual central island of vision, with reduced visual acuities (e.g., 20/50 in patient III-8, at age 58 years). Records from two other affected males (IV-1 and IV-2), who are in their 4th decade of life, described "RP" on clinical examination, with severely limited visual fields, and retained visual acuity.

Standard ERGs are shown for young male patients at different disease stages (fig. 3*B*). Patient V-1 had a reduced but recordable rod b-wave, to dim blue flashes of light in the dark-adapted state. A bright white (maximal standard) flash elicited a negative waveform, with reduced a- and b-wave amplitudes. Cone ERGs were normal in amplitude and timing. Patient IV-3 had no detectable rod b-wave, reduced a- and b-wave amplitudes to a maximal stimulus, and cone ERGs that were reduced in amplitude and delayed in timing. Patient III-8 (age 58 years) had no detectable ERGs with these stimuli. The natural history of cone flicker ERG-amplitude loss in patients IV-3 and IV-4, over a decade of serial observations, indicates an average loss of 0.1 log unit (21%) of remaining cone flicker ERG amplitude per year.

Figure 3*C* shows ERGs described by use of a model

**Table 1**

**Two-Point LOD Scores between *RP24* and Marker Loci Spanning Xp22.32-11.23**

| | | LOD Score at $\theta$ = | | | | | | | |
|---|---|---|---|---|---|---|---|---|---|
| Locus[a] | $Z_{max}$ ($\theta$) | .00 | .01 | .05 | .10 | .20 | .30 | .40 | .50 |
| KAL | .000 (.500) | −∞ | −7.69 | −4.28 | −2.86 | −1.52 | −.78 | −.31 | .00 |
| DXS989 | .000 (.500) | −∞ | −9.43 | −5.29 | −3.54 | −1.87 | −.97 | −.39 | .00 |
| DXS1214 | .000 (.500) | −∞ | −4.08 | −2.27 | −1.44 | −.69 | −.32 | −.12 | .00 |
| CYBB | .000 (.500) | −∞ | −3.96 | −1.96 | −1.18 | −.50 | −.19 | −.05 | .00 |
| DXS1068 | .000 (.500) | −∞ | −7.29 | −3.88 | −2.47 | −1.17 | −.52 | −.17 | .00 |
| DXS7 | .002 (.473) | −2.71 | −2.39 | −1.30 | −.77 | −.31 | −.10 | −.01 | .00 |
| MAOB | .000 (.500) | −∞ | −5.68 | −2.99 | −1.92 | −.93 | −.43 | −.14 | .00 |
| DXS1003 | .000 (.500) | −∞ | −4.62 | −3.40 | −2.85 | −1.43 | −.59 | −.16 | .00 |
| DXS1367 | .000 (.500) | −∞ | −7.02 | −4.67 | −3.14 | −1.57 | −.75 | −.26 | .00 |
| DXS6849 | .000 (.500) | −∞ | −5.03 | −3.73 | −2.79 | −1.36 | −.60 | −.19 | .00 |
| DXS6941 | .035 (.424) | −∞ | −3.66 | −1.69 | −.94 | −.32 | −.06 | .03 | .00 |

[a] The order of the loci is from pter to cen.

of phototransduction in a normal subject and in patient V-1 and a graphical summary of parameters for three affected individuals. ERGs evoked by two different intensities of blue flashes (upper and lower traces) and a red flash (middle trace) are shown; the upper two traces are scotopically matched, and the lower two traces are photopically matched. The rod (dashed lines) and cone (dotted lines) components of the phototransduction model are estimated to fit the sum (thick solid line) to the three ERG traces simultaneously (Cideciyan et al. 1998). The ERG of patient V-1, evoked by a bright blue flash, dark adapted, lacked a b-wave. $R_{max}$ and sensitivity (log $\sigma$) parameters for rods and cones are plotted as the logarithm of the ratio to the mean normal; rectangles show the normal range. Rod $R_{max}$ was reduced, but sensitivity was normal for patient V-1; cone $R_{max}$ and sensitivity fell within normal limits. Patients IV-3 and IV-4 were tested in light-adapted conditions, to obtain cone photoresponses; $R_{max}$ and sensitivity are plotted with respect to corresponding mean normals. These two affected males had reduced cone $R_{max}$, with normal sensitivity.

Females who are obligate heterozygotes by history were not symptomatic. Patient III-7 showed, by perimetry, patchy rod and cone sensitivity losses in both eyes and abnormalities of rod and cone ERGs that are similar to those reported for females who are obligate carriers of XLRP (e.g., see Berson et al. 1979; Fishman et al. 1986; Jacobson et al. 1989).

## Discussion

We have localized a novel locus (*RP24*) for XLRP to Xq26-27, within a 23-cM region, by using extensive haplotype and linkage analyses. So far, other XLRP loci have been mapped only to Xp. The assertion that *RP3* is the predominant XLRP locus (accounting for 70% of families) is based on heterogeneity tests, but, interestingly, only 20% of affected families reveal causative mutations in the *RPGR* gene from the RP3 region. For most pedigrees, it is difficult to distinguish between XLRP subtypes, because of the small size of the pedigrees and the short genetic interval (10–20 cM) that separates the *RP3* and *RP2* loci at Xp. In earlier studies, markers spanning most of the Xq chromosomal region had not been employed for genetic analysis of affected families. This is the first study in which the entire X chromosome was scanned for linkage to the disease locus, and, although the pedigree studied is not very large, we were able to obtain a significant LOD score of >4 with DXS8106 at Xq26-27. The mapping of *RP24* should lead to reevaluation of genetic data, with additional markers and for a larger cohort of XLRP families.

Phenotype analyses of affected male individuals with XLRP have suggested that rod photoreceptors are an early site of disease manifestation. In one young hemizygote from the RP24 family who had normal cone function, there was not only rod photoreceptor outer-segment disease but also disproportionate loss of rod bipolar cell activity. Whether the functional abnormality at or proximal to the rod synapse is a direct manifestation of the defective gene product or a secondary degenerative process requires further investigation. "Negative ERGs" have been noted for other forms of RP (e.g., see Cideciyan and Jacobson 1993), and rod synaptic changes have been found in transgenic animals with primary rod photoreceptor outer-segment disease (e.g., see Roof et al. 1994; Li et al. 1998). The natural history of RP24 disease involves progressive loss of both rod and cone receptor and postreceptor function, with relative preservation of central versus peripheral function and, eventually, severe retinal degeneration.

A large number of retinal diseases have been localized to the X chromosome, but only a few map to Xq (see fig. 2). Recently, a gene for an X-linked cone dystrophy (*COD2*) was assigned to Xq27, in an 8-cM genetic in-

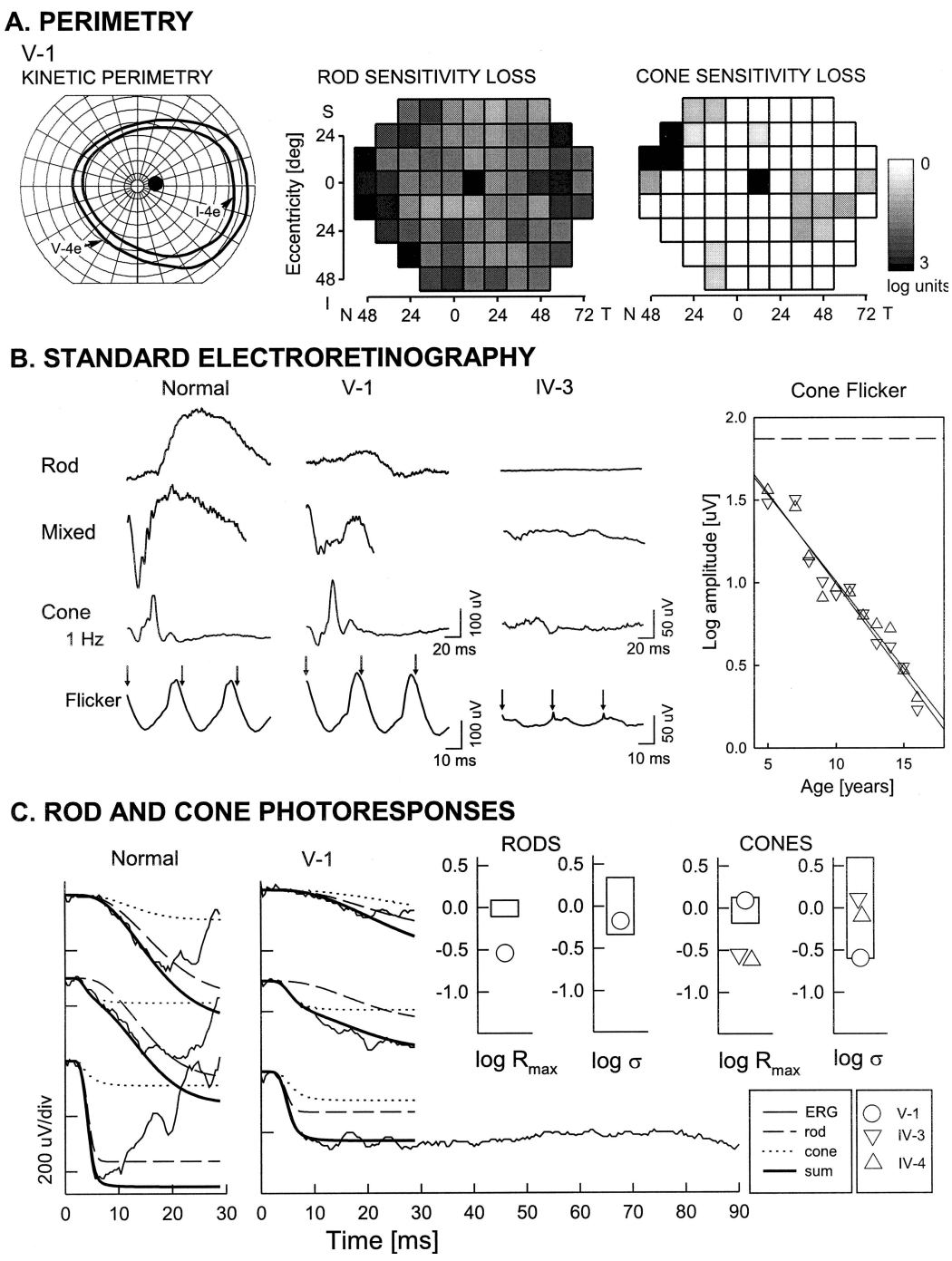


**Figure 3** Results of visual-function tests of young males. *A,* Kinetic perimetry and static threshold perimetry for V-1, at age 11 years. Static perimetry is displayed as gray-scale maps of rod and cone sensitivity loss: white indicates normal, and black indicates >3 log units of sensitivity loss for rods and unmeasurable sensitivity for cones; the physiological blind spot is shown as black, at the 12° temporal ("T") field. N = nasal, I = inferior, and S = superior. *B,* Rod, mixed, and cone ERGs for a representative normal subject and for V-1 (age 11 years) and IV-3 (age 14 years). Stimulus onset is at trace onset. Arrows indicate stimulus onset for 30-Hz flicker in the presence of a background; calibration bars are shown. Serial cone flicker ERG amplitudes for two hemizygotes were recorded in the absence of a background and with a 0.7–log unit dimmer stimulus, compared with standard traces; the dashed line indicates the mean normal amplitude. *C,* Photoresponses (*thin solid lines*) to blue (2.3 and 4.6 log scot.td.s, upper and lower traces, respectively) and red (3.6 log phot.td.s, middle trace) stimuli in the dark-adapted state, for a representative normal subject and affected male V-1. Rod (*dashed lines*) and cone (*dotted lines*) components of the phototransduction activation model and their sum (*thick solid line*) are shown. Parameters of rod and cone activation are plotted for V-1, IV-3, and IV-4 (ages 11, 15, and 15 years, respectively); boxes represent normal limits.

**Table 2**

**Two-Point LOD Scores between *RP24* and Marker Loci Spanning Xq25-28**

| | | LOD Score at $\theta$ = | | | | | | | |
|---|---|---|---|---|---|---|---|---|---|
| Locus[a] | $Z_{max}$ ($\theta$) | .00 | .01 | .05 | .10 | .20 | .30 | .40 | .50 |
| DXS1046 | 1.432 (.147) | −∞ | −.13 | 1.05 | 1.37 | 1.38 | 1.08 | .61 | .00 |
| DXS8094 | 2.132 (.071) | −∞ | 1.64 | 2.10 | 2.11 | 1.78 | 1.28 | .69 | .00 |
| DXS1211 | 2.966 (.000) | 2.97 | 2.92 | 2.72 | 2.46 | 1.92 | 1.34 | .70 | .00 |
| DXS1192 | 3.612 (.000) | 3.61 | 3.56 | 3.32 | 3.02 | 2.35 | 1.61 | .81 | .00 |
| DXS984 | .601 (.000) | .60 | .59 | .55 | .50 | .39 | .27 | .14 | .00 |
| DXS1232 | 1.204 (.000) | 1.20 | 1.18 | 1.09 | .98 | .72 | .44 | .17 | .00 |
| DXS8013 | 2.782 (.000) | 2.78 | 2.73 | 2.53 | 2.26 | 1.71 | 1.10 | .44 | .00 |
| DXS1205 | 2.819 (.000) | 2.82 | 2.77 | 2.55 | 2.28 | 1.69 | 1.08 | .49 | .00 |
| DXS1227 | 1.505 (.000) | 1.50 | 1.48 | 1.37 | 1.23 | .93 | .59 | .25 | .00 |
| DXS8106 | 4.214 (.000) | 4.21 | 4.15 | 3.88 | 3.53 | 2.76 | 1.91 | .96 | .00 |
| DXS8084 | 3.656 (.000) | 3.66 | 3.59 | 3.34 | 3.02 | 2.31 | 1.53 | .73 | .00 |
| DXS8043 | 2.618 (.066) | −∞ | 2.15 | 2.60 | 2.57 | 2.16 | 1.54 | .79 | .00 |
| DXS8011 | 1.656 (.134) | −∞ | .16 | 1.32 | 1.62 | 1.56 | 1.17 | .61 | .00 |

[a] The order of the loci is from cen to qter.

terval between DXS292 and DXS1113 (Bergen and Pinckers 1997). This interval has a partial overlap with the *RP24* critical region that we have reported. For the RP24 family, retinal function and clinical results are completely different from those described for the COD2 family. Nevertheless, it is conceivable that RP24 and COD2 are allelic diseases. This hypothesis can be tested after cloning of either of the responsible genes.

At this stage, the critical region of the *RP24* locus (i.e., the region between DXS8094 and DXS8043) spans 23 cM. We plan to explore additional families unlinked to Xp loci and/or genotype more members of the XLRP-114 family, to narrow the genetic interval. A positional candidate approach will also be employed to facilitate *RP24* cloning. The genes for Lowe oculocerebrorenal syndrome and for red and green cone pigments (RCP and GCP, respectively) reside outside the *RP24* critical region. A search of the human expressed-sequence database at the National Center for Biotechnology Information revealed six genes and 10 unidentified transcripts (expressed-sequence tags [ESTs]) within a 24-cM region that includes the *RP24* interval. Of the six genes, only one (cerebellar degeneration–associated protein mRNA [*CDR34*]; Chen et al. 1990) appears to be a good candidate and will be examined for mutation(s) in the RP24 family. Among the 10 ESTs, 7 have been isolated from human brain (infant or adult) cDNA libraries and may be suitable as candidate genes. Elucidation of the molecular and biochemical defect(s) at the *RP24* locus promises to provide significant insights into visual function and to facilitate further development of diagnostic and therapeutic approaches for XLRP.

## Acknowledgments

We are grateful to D. Hanna, L. Gardner, J. Christopher, K. Mejia, and H. Heo for help with the study; to Y. Huang and K. Zhao for data analyses; and to D. Giebel for assistance in preparing the manuscript. This research was supported by grants from the National Institutes of Health (EY07961 to A.S., EY05627 to S.G.J., EY05235 to D.G.B., and HG00008 to J.O.), the Foundation Fighting Blindness (to A.S., A.V.C., D.G.B., D.R.H., J.O., and S.G.J.), the Chatlos Foundation, Inc. (to S.G.J.), the Food and Drug Administration (to D.R.H.), the Kirby Foundation (to S.G.J), the Mackall Trust (to S.G.J.), the Whitaker Foundation (to A.V.C.), and by unrestricted departmental support from Research to Prevent Blindness. We also acknowledge National Institutes of Health grants EY07003 (Core) and M01-RR00042 (General Clinical Research Center) and a Shared Equipment grant from the Office of the Vice President for Research, University of Michigan. A.S. is the recipient of a Research to Prevent Blindness Lew R. Wasserman Merit Award.

## Electronic-Database Information

URLs for data in this article are as follows:

Généthon, http://www.genethon.fr (for descriptions of the polymorphic markers, genetic distances, and PCR conditions used)

Genome Database, http://gdbwww.gdb.org (for descriptions of the polymorphic markers, genetic distances, and PCR conditions used)

National Center for Biotechnology Information, http://www4.ncbi.nlm.nih.gov (for descriptions of mapped genes and ESTs)

Online Mendelian Inheritance in Man (OMIM), http://www.ncbi.nlm.nih.gov/Omim (for map locations of loci for RP, macular degeneration, and other retinal diseases and for markers)

RetNet, http://www.sph.uth.tmc.edu/RetNet (for map locations of loci for RP, macular degeneration, and other retinal diseases)

## References


Aldred MA, Jay M, Wright AF (1994*a*) X-linked retinitis pigmentosa. In: Wright AF, Jay B (eds) Molecular genetics of inherited eye disorders. Harwood Academic Publishers, Chur, Switzerland, pp 259–276

Aldred MA, Teague PW, Jay M, Bundey S, Redmond RM, Jay B, Bird AC, et al (1994*b*) Retinitis pigmentosa families showing apparent X linked inheritance but unlinked to the RP2 or RP3 loci. J Med Genet 31:848–852

Becker A, Geiger D, Schaffer AA (1998) Automatic selection of loop breakers for genetic linkage analysis. Hum Hered 48:49–60

Bergen AAB, Pinckers AJLG (1997) Localization of a novel X-linked progressive cone dystrophy gene to Xq27: evidence for genetic heterogeneity. Am J Hum Genet 60:1468–1473

Berson EL, Rosen JB, Simonoff EA (1979) Electroretinographic testing as an aid in detection of carriers of X-chromosome–linked retinitis pigmentosa. Am J Ophthalmol 87: 460–468

Bhattacharya SS, Wright AF, Clayton JF, Price WH, Phillips CI, McKeown CME, Jay M, et al (1984) Close genetic linkage between X-linked retinitis pigmentosa and a restriction fragment length polymorphism identified by recombinant DNA probe L1.28. Nature 309:253–255

Birch DG, Fish GE (1987) Rod ERGs in retinitis pigmentosa and cone-rod degeneration. Invest Ophthalmol Vis Sci 28: 140–150

Buraczynska M, Wu W, Fujita R, Buraczynska K, Phelps E, Andreasson S, Bennett J, et al (1997) Spectrum of mutations in the *RPGR* gene that are identified in 20% of families with X-linked retinitis pigmentosa. Am J Hum Genet 61: 1287–1292

Chen YT, Rettig WJ, Yenamandra AK, Kozak CA, Chaganti RSK, Posner JB, Old LJ (1990) Cerebellar degeneration–related antigen: a highly conserved neuroectodermal marker mapped to chromosomes X in human and mouse. Proc Natl Acad Sci USA 87:3077–3081

Cideciyan AV, Hood DC, Huang Y, Banin E, Li Z-Y, Stone EM, Milam AH, et al (1998) Disease sequence from mutant rhodopsin allele to rod and cone photoreceptor degeneration in man. Proc Natl Acad Sci USA 95:7103–7108

Cideciyan AV, Jacobson SG (1993) Negative electroretinograms in retinitis pigmentosa. Invest Ophthalmol Vis Sci 34: 3253–3263

——— (1996) An alternative phototransduction model for human rod and cone ERG a-waves: normal parameters and variation with age. Vision Res 36:2609–2621

Fishman GA, Farber MD, McMahon TT (1986) X-linked retinitis pigmentosa: clinical characteristics of carriers. Arch Ophthalmol 104:1329–1335.

Fujita R, Buraczynska M, Gieser L, Wu W, Forsythe P, Abrahamson M, Jacobson SG, et al (1997) Analysis of the *RPGR* gene in 11 pedigrees with the retinitis pigmentosa type 3 genotype: paucity of mutations in the coding region but splice defects in two families. Am J Hum Genet 61:571–580

Fujita R, Swaroop A (1996) RPGR: part one of the X-linked retinitis pigmentosa story. Mol Vis 2:4, http://www.molvis.org/molvis/v2/fujita

Heckenlively JR (1988) Retinitis pigmentosa. Lippincott, Philadelphia

Hood DC, Birch DG (1993) Light adaptation of human receptors: the leading edge of the human a-wave and models of receptor activity. Vision Res 33:1605–1618

——— (1995) Phototransduction in human cones measured using the a-wave of the ERG. Vision Res 35:2801–2810

——— (1997) Assessing abnormal rod photoreceptor activity with the a-wave of the electroretinogram: applications and methods. Doc Ophthalmol 92:253–267

Jacobson SG, Apathy PP, Parel JM (1991) Rod and cone perimetry: computerized testing and analysis. In: Heckenlively J, Arden G (eds) Handbook of clinical vision testing. Mosby Year Book, St Louis, pp 475–482

Jacobson SG, Buraczynska M, Milam AH, Chen C, Jarvalainen M, Fujita R, Wu W, et al (1997) Disease expression in X-linked retinitis pigmentosa caused by a putative null mutation in the *RPGR* gene. Invest Ophthalmol Vis Sci 38: 1983–1997

Jacobson SG, Yagasaki K, Feuer WJ, Roman A (1989) Interocular asymmetry of visual function in heterozygotes of X-linked retinitis pigmentosa. Exp Eye Res 48:679–691

Lathrop GM, Lalouel J-M, Julier C, Ott J (1984) Strategies for multilocus analysis in humans. Proc Natl Acad Sci USA 81:3443–3446

Li Z-Y, Wong F, Chang JH, Possin DE, Hao Y, Petters RM, Milam AH (1998) Rhodopsin transgenic pigs as a model for human retinitis pigmentosa. Invest Ophthalmol Vis Sci 39:808–819

McGuire RE, Sullivan LS, Blanton SH, Church MW, Heckenlively JR, Daiger SP (1995) X-linked dominant cone-rod degeneration: linkage mapping of a new locus for retinitis pigmentosa (RP15) to Xp22.13-p22.11. Am J Hum Genet 57:87–94

Meindl A, Dry K, Herrmann K, Manson F, Ciccodicola A, Edgar A, Carvalho MRS, et al (1996) A gene (RPGR) with homology to the RCC1 guanine nucleotide exchange factor is mutated in X-linked retinitis pigmentosa (RP3). Nat Genet 13:35–42

Musarella MA, Anson-Cartwright L, Leal SM, Gilbert LD, Worton RG, Fishman GA, Ott J (1990) Multipoint linkage analysis and heterogeneity testing in 20 X-linked retinitis pigmentosa families. Genomics 8:286–296

Ott J, Bhattacharya SS, Chen JD, Denton MJ, Donald J, Dubay C, Farrar GJ, et al (1990) Localizing multiple X-chromosome–linked retinitis pigmentosa loci using multilocus homogeneity tests. Proc Natl Acad Sci USA 87:701–704

Roepman R, van Duijnhoven G, Rosenberg T, Pinckers AJLG, Bleeker-Wagemakers LM, Bergen AAB, Post J, et al (1996) Positional cloning of the gene for X-linked retinitis pigmentosa 3: homology with the guanine-nucleotide–exchange factor RCC1. Hum Mol Genet 5:1035–1041

Roof DJ, Adamian M, Hayes A (1994) Rhodopsin accumulation at abnormal sites in retinas of mice with a human P23H rhodopsin transgene. Invest Ophthalmol Vis Sci 35: 4049–4062

Schwahn U, Lenzner S, Dong J, Feil S, Hinzmann B, van Duijnhoven G, Kirschner R, et al (1998) Positional cloning of the gene for X-linked retinitis pigmentosa 2. Nat Genet 19: 327–332

Teague PW, Aldred MA, Jay M, Dempster M, Harrison C, Carothers AD, Hardwick LJ, et al (1994) Heterogeneity analysis in 40 X-linked retinitis pigmentosa families. Am J Hum Genet 55:105–111

Terwilliger JD, Ott J (1994) Handbook of human genetic linkage. Johns Hopkins University Press, Baltimore

Thiselton DL, Hampson RM, Nayudu M, Maldergem LV, Wolf ML, Saha BK, Bhattacharya SS, et al (1996) Mapping the RP2 locus for X-linked retinitis pigmentosa on proximal Xp: a genetically defined 5-cM critical region and exclusion of candidate genes by physical mapping. Genome Res 6: 1093–1102